
EXPLOIT WHERE OPTIMIZER EXPLORES VIA RESIDUALS

A PREPRINT

An Xu, Zhouyuan Huo, Heng Huang
 Department of Electrical and Computer Engineering
 University of Pittsburgh
 {an.xu, zhouyuan.huo, heng.huang}@pitt.edu

Jun 5, 2020

ABSTRACT

In order to train the neural networks faster, many efforts have been devoted to exploring a better solution trajectory, but few have been put into exploiting the existing solution trajectory. To exploit the trajectory of (momentum) stochastic gradient descent (SGD(m)) method, we propose a novel method named SGD(m) with residuals (RSGD(m)), which leads to a performance boost of both the convergence and generalization. Our new method can also be applied to other optimizers such as ASGD and Adam. We provide theoretical analysis to show that RSGD achieves a smaller growth rate of the generalization error and the same (but empirically better) convergence rate compared with SGD. Extensive deep learning experiments on image classification, language modeling and graph convolutional neural networks show that the proposed algorithm is faster than SGD(m)/Adam at the initial training stage, and similar to or better than SGD(m) at the end of training with better generalization error.

1 Introduction

Stochastic Gradient Descent and its momentum variants have been the most common methods in training deep neural networks for computer vision applications. Other adaptive optimization methods, *e.g.* AdaGrad [7], RMSprop [29], and Adam [15], feature a fast initial training phase. But their convergence and generalization performance quickly deteriorate compared with the non-adaptive counterparts. In this paper, instead of developing another optimization variant method to *explore* a faster solution trajectory, we show that we can *exploit* the existing solution trajectory to obtain **a much better solution nearby** during training. In reinforcement learning, **exploration refers to gathering more information, while exploitation refers to finding the best solution based on the current information**. We focus on the under-exploited nature of the widely used deep learning optimization methods: (momentum) stochastic gradient descent (SGD(m) for short). More specifically, provided with the solution trajectory of base optimizers including SGD(m), can we unearth its potentials via proper exploitation in the proximity?

To address this novel and important problem, we propose a new (momentum) stochastic gradient descent with residuals (RSGD(m)) algorithm, in which the SGD(m) solution trajectory is regarded as the reference and the residual scheme is introduced to conduct the exploitation in the proximity of the reference. We summarize our contributions as follows:

- We propose a novel RSGD(m) algorithm. There is no need to tune any hyperparameters of the base optimizer. Our method enables the optimizer to exploit the proximity of the solution trajectory to improve the convergence and generalization performance.
- Three residual schemes - scaling, scaled sign and top-k schemes - are explored in this paper. We conduct theoretical convergence and generalization analysis of the scaling scheme. A *trade-off* exists in the exploitation.
- Extensive experiments show substantial improvement on the convergence and generalization performance of the proposed method. In LSTM and Cluster-GCN [6] tasks, we also apply our techniques to ASGD [23] and Adam, respectively.

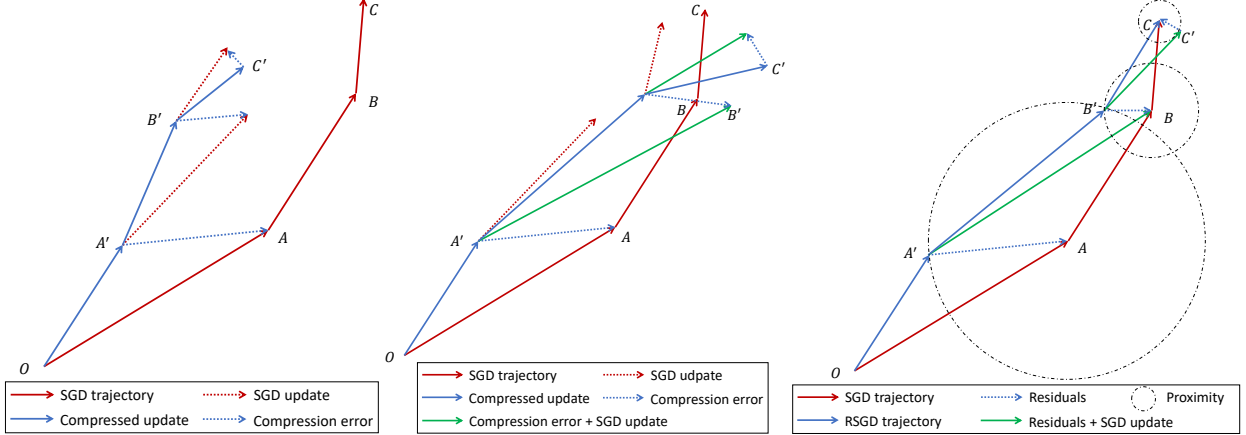


Figure 1: Sketches of the solution trajectory ($O \rightarrow A/A' \rightarrow B/B' \rightarrow C/C' \rightarrow \dots$), where O is the initialization point. Left: gradient compression. Middle: error feedback. Right: RSGD.

2 Related Works

Residuals Residuals have been incorporated in communication-efficient distributed training with compressed gradients. But it only compensates for the performance loss. Gradient compression includes quantization and sparsification. In gradient quantization, the worker nodes send gradients of low bits to the master node. An aggressive way is to represent the gradient with its sign (SignSGD) [3, 4]. Throughout this paper, we refer to scaled SignSGD as the scaled sign scheme:

$$\mathcal{R}(\mathbf{x}) = \frac{\|\mathbf{x}\|_1}{d} \cdot \text{sign}(\mathbf{x}), \quad (1)$$

where $\mathbf{x} \in \mathbb{R}^d$ is the vector to compress. Gradient sparsification is another compression technique to reduce the non-zero gradient component to be sent to the master. The worker nodes can either select top k components of the gradient [27, 1, 26, 2] or each component with a probability to keep the unbiasedness [30].

Nevertheless, gradient compression can jeopardize performance. Local error accumulation and feedback [19, 13, 33] were proposed to reduce the loss of performance. Specifically, it adds the current compression error into the gradient of the next training iteration. Shown by the left of Figure 1, gradient compression introduces error at each training step and deviates from the SGD trajectory. Although error feedback alleviates this effect as shown in the middle of Figure 1, it does not strictly follow the SGD trajectory, leading to potentially worse performance.

Generalization The theoretical analysis of the generalization of RSGD incorporates the uniform stability approach. Uniform stability was first proposed in [5], focusing on the inherent stability property of the learning algorithm. [5] analyzed bagging methods. It was later utilized to analyze the generalization property of SGD [8] and its momentum variants [31]. [18] established a data-dependent notion of the stability to stress the distribution-dependent risk of the initialization point and make the generalization bounds more optimistic.

3 Preliminaries

Assume that all the samples in the training dataset $S = \{z_i\}_{i=1}^N$ are *i.i.d.* sampled from the sample space \mathcal{Z} . The training dataset size $|S| = N$. The loss function of the sample z is $f(\mathbf{x}, z)$, where the model parameters $\mathbf{x} \in \mathbb{R}^d$. We denote the partial gradients $\frac{\partial f(\mathbf{x}, z)}{\partial \mathbf{x}}$ as $\nabla f(\mathbf{x}, z)$. The goal is to solve the population risk minimization problem (PRM) as following:

$$\min_{\mathbf{x} \in \mathbb{R}^d} R(\mathbf{x}) := \mathbb{E}_{z \sim \mathcal{Z}} f(\mathbf{x}, z). \quad (2)$$

However, the population risk $R(\mathbf{x})$ is computationally undesirable in practice. Under the *i.i.d.* sampling condition, we usually solve the empirical risk minimization problem (ERM) as an alternative:

$$\min_{\mathbf{x} \in \mathbb{R}^d} R_S(\mathbf{x}) := \frac{1}{N} \sum_{i=1}^N f(\mathbf{x}, z_i). \quad (3)$$

Algorithm 1 (Momentum) Stochastic Gradient Descent with Residuals (RSGD(m)).

Input: training dataset S , number of iterations T , learning rate $\{\gamma_t\}_{t=0}^{T-1}$, parameters \mathbf{x}_0 , residual scheme \mathcal{R} and the momentum constant m .
Initialize: initial residuals $\mathbf{r}_0 = \mathbf{0}$ and momentum buffer $\mathbf{v}_0 = \mathbf{0}$.
for $t = 0$ to $T - 1$ **do**
 Randomly pick a sample z_t from S .
 $\mathbf{v}_{t+1} = m \cdot \mathbf{v}_t + \nabla f(\mathbf{x}_t - \mathbf{r}_t, z_t)$ // SGD(m).
 $\mathbf{x}_{t+\frac{1}{2}} = \mathbf{x}_t - \mathbf{r}_t - \gamma_t \cdot \mathbf{v}_{t+1}$ // Residual schemes.
 $\hat{\mathbf{r}}_t = \mathcal{R}(\mathbf{x}_t - \mathbf{x}_{t+\frac{1}{2}})$ // Re-descent.
 $\mathbf{x}_{t+1} = \mathbf{x}_t - \hat{\mathbf{r}}_t$ // Update residuals.
 $\mathbf{r}_{t+1} = \mathbf{x}_t - \mathbf{x}_{t+\frac{1}{2}} - \hat{\mathbf{r}}_t$
end for
Output: parameters \mathbf{x}_T

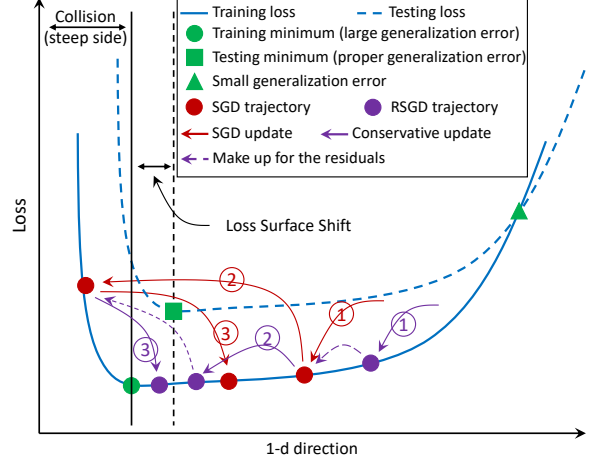


Figure 2: A sketch of the loss projected to a 1-d direction. A proper decrease of generalization error improves the performance.

The **generalization error** is defined as $R_s(\mathbf{x}) - R(\mathbf{x})$. Consider the learning algorithm A (usually iterative and randomized) as a map: $S \rightarrow \Re^d$. Let $S' = \{z'_i\}_{i=1}^N$ be another dataset and *i.i.d.* sampled from \mathcal{Z} . For the model parameters trained on S with A , the population risk satisfies $R(A(S)) = \mathbb{E}_{S',A} \left(\frac{1}{N} \sum_{i=1}^N f(A(S), z'_i) \right)$. We denote $S'^{(i)}$ as $\{z_1, \dots, z_{i-1}, z'_i, z_{i+1}, \dots, z_N\}$ differing from the training dataset S with one sample z'_i at most. The uniform stability is defined as follows.

Definition 1 (Uniform stability) The randomized algorithm A has ϵ -uniform stability if $\forall i \in \{1, 2, \dots, N-1\}, z \in \mathcal{Z}$ and $S, S'^{(i)} \in \mathcal{Z}^N$, we have $\mathbb{E}_A[f(A(S), z) - f(A(S'^{(i)}), z)] \leq \epsilon$.

The uniform stability ϵ also bounds the expected generalization error as shown in Theorem 1. Consequently, we leverage the uniform stability approach for generalization analysis.

Theorem 1 ([8]) If the randomized algorithm A is ϵ -uniform stable, then $|\mathbb{E}_{S,A}[R_S(A(S)) - R(A(S))]| \leq \epsilon$.

4 New SGD(m) with Residuals Algorithm

In this section, we propose the RSGD(m) algorithm (summarized in Algorithm 1), the trajectory of which is visualized at the right of Figure 1. The existing SGD(m) algorithm has been widely used in computer vision tasks.

4.1 Reference Trajectory

The reference SGD(m) trajectory $\{\mathbf{x}_{t-\frac{1}{2}}\}_{t=0}^{T-1} (\mathbf{x}_{-\frac{1}{2}} := \mathbf{x}_0)$ is the key to the guaranteed convergence performance of RSGD(m) compared with SGD(m). When employing residuals (the right of Figure 1), the update direction always aims at the reference trajectory point $\mathbf{x}_{t+\frac{1}{2}}$ at the next training step, which is not guaranteed in gradient compression with or without error feedback. We first subtract current residuals \mathbf{r}_t from \mathbf{x}_t to reach the current reference trajectory point $\mathbf{x}_{t-\frac{1}{2}}$. Then a stochastic gradient $\nabla f(\mathbf{x}_t - \mathbf{r}_t, z_t)$ is computed to reach the next reference trajectory point $\mathbf{x}_{t+\frac{1}{2}}$. With the current RSGD(m) parameters \mathbf{x}_t and the next SGD(m) parameters $\mathbf{x}_{t+\frac{1}{2}}$, we can reach the next RSGD(m) parameters \mathbf{x}_{t+1} using various residual schemes \mathcal{R} (refer to Algorithm 1).

The RSGD(m) trajectory $\{\mathbf{x}_t\}_{t=0}^{T-1}$ will always be around the SGD(m) reference trajectory $\{\mathbf{x}_{t-\frac{1}{2}}\}_{t=0}^{T-1}$ if using proper residual schemes. This leads to an additional error term in the convergence analysis, but it can be empirically beneficial.

4.2 Exploitation in the Proximity

We elaborate this as the exploitation in the proximity of the reference trajectory. The radius of the proximity can be defined as $\|\mathbf{x}_t - \mathbf{x}_{t-\frac{1}{2}}\|$ and determines the degree of the exploitation. It becomes a **trade-off** because the larger the radius of the proximity is, the more RSGD(m) can exploit but also the smaller the probability that RSGD(m) can find a better result is. Consequently, a proper residual scheme needs to consider both. We theoretically support the trade-off at the end of section 6 via combining the convergence and generalization analysis of the scaling residual scheme with Figure 2.

4.3 Residual Schemes

We mainly consider three residual schemes. The first is the scaling scheme $\mathcal{R}(\mathbf{x}) = \alpha \mathbf{x}$, where α is the scaling factor. We assume $0 < \alpha < 1$, because $\alpha = 1$ corresponds to zero residuals and $\alpha = 0$ implies zero updating of the parameters. The scaling factor α affects the radius of the exploitation proximity. A smaller α indicates larger proximity. Via properly decreasing α the performance can be improved, but decreasing α even further can be counterproductive. The extreme circumstance is that when α is infinitely close to 0, there will be barely any updating of the model parameters and the training will be hard to converge.

The second is the scaled sign scheme as shown in Eq. (1), which is motivated by the need for gradient compression in communication-efficient distributed training. Note that the purpose of RSGD(m) with the sign residual scheme (RSGD(m)-sign for short) is different from error feedback (EF-SignSGD(m)) as mentioned in Section 2. RSGD(m)-sign tries to improve SGD(m) with the sign residual scheme, while EF-SignSGD(m) only compensates for the performance loss due to quantization. The third is the top-k scheme, which sparsifies the gradient by only selecting the largest k components.

4.4 Collision Avoidance

As one may still wonder why residual schemes can be a good practice to exploit the proximity, we elaborate it with an intuitive explanation from the view of the loss surface illustrated by Figure 2.

Flat local minimum. SGD-related method converges to flat local minima [14, 16]. Flat minima are more robust to the shift between training loss and testing loss surface, thus it generalizes better than sharp local minima [14, 12, 9].

Dangerous zone. Although flat local minima are more desirable than sharp local minima, the solutions SGD found are biased toward the steep side of the flat local minima [12]. We name the area around the steep side of the flat local minimum as "dangerous zone" because 1) collision to the steep side leads to a much worse training/testing performance; 2) it is vulnerable to the shift of testing loss surface. Note that **the dangerous zone exists not only after convergence, but also during training and along the solution trajectory** (Figure 6 in [9] shows that the biased solutions towards the steep side exist during training). This gives the motivation to avoid the dangerous zone during training via proper exploitation in the proximity of the solution trajectory.

Conservative update. "Residual" schemes lead to a conservative version of the original gradients. It is significantly different from using a small learning rate which affects the reference solution trajectory. Specifically, the scaling scheme reduces the gradient value, the scaled sign scheme reduces large gradient components, and the topk scheme removes some gradient components. The conservative update with residual schemes reduces the chance of RSGD trajectory entering the dangerous zone and colliding to the steep side as shown by Figure 2. This can lead to smaller testing loss during training.

5 Convergence Analysis

Theorem 2 *The reference trajectory $\{\mathbf{x}_{t-\frac{1}{2}}\}_{t=0}^{T-1}$ follows the stochastic gradient descent scheme due to $\mathbf{x}_{t+1-\frac{1}{2}} = \mathbf{x}_{t-\frac{1}{2}} - \gamma_t \nabla f(\mathbf{x}_{t-\frac{1}{2}}, z_t)$.*

Assumption 1 (β -smooth) $\forall \mathbf{x}, \mathbf{y} \in \mathbb{R}^d$, we have $\|\nabla R_S(\mathbf{x}) - \nabla R_S(\mathbf{y})\| \leq \beta \|\mathbf{x} - \mathbf{y}\|$. It also implies $R_S(\mathbf{x}) - R_S(\mathbf{y}) \leq \langle \nabla R_S(\mathbf{y}), \mathbf{x} - \mathbf{y} \rangle + \frac{\beta}{2} \|\mathbf{x} - \mathbf{y}\|^2$.

Assumption 2 (Bounded second moment) $\forall \mathbf{x} \in \mathbb{R}^d$, the stochastic gradient satisfies: $\mathbb{E}_{z \sim S} \|\nabla f(\mathbf{x}, z)\|^2 \leq \sigma^2$.

Assumption 3 (Unbiasedness) $\forall \mathbf{x} \in \mathbb{R}^d$, the stochastic gradient satisfies: $\mathbb{E}_{z \sim S} [\nabla f(\mathbf{x}, z)] = \nabla R_S(\mathbf{x})$.

Theorem 3 (*Convergence of RSGD*) Assume R_S is non-convex and Assumption 1, 2 and 3 exist. For the fixed learning rate γ and for all $c_1 > 0$, we have $\min_{0 \leq t \leq T-1} \mathbb{E} \|\nabla R_S(\mathbf{x}_t)\|_2^2 \leq \frac{(1+c_1)(R_S(\mathbf{x}_0) - R_S(\mathbf{x}_*))}{\gamma T} + \frac{(1+c_1)\beta\gamma\sigma^2}{2} + (1 + \frac{1}{c_1})\beta^2 \frac{\sum_{t=0}^{T-1} \mathbb{E} \|\mathbf{r}_t\|_2^2}{T}$.

In Theorem 3, the last error term is closely related to the residual scheme. The convergence rate is the same $\mathcal{O}(\frac{1}{\sqrt{T}})$ as SGD if using proper schemes. Current convergence analysis of SGDM [32]/Local SGD [25]/Adam [15] also show the same convergence rate, but they are empirically faster than SGD.

Corollary 3.1 (*Convergence of RSGD-scale*) Consider the scaling residual scheme $\mathcal{R}(\mathbf{x}) = \alpha \mathbf{x}$ based on the specifications of Theorem 3, where the scaling factor α satisfies $0 < \alpha < 1$. For all $c_2 > 0$ and $(1-\alpha)^2(1+c_2) < 1$. When the number of iterations T is large enough, we have $\min_{0 \leq t \leq T-1} \mathbb{E} \|\nabla R_S(\mathbf{x}_t)\|_2^2 \leq \frac{(1+c_1)(R_S(\mathbf{x}_0) - R_S(\mathbf{x}_*))}{\gamma T} + \frac{(1+c_1)\beta\gamma\sigma^2}{2} + \frac{(1-\alpha)^2(1+\frac{1}{c_2})(1+\frac{1}{c_1})}{1-(1-\alpha)^2(1+c_2)} \beta^2 \gamma^2 \sigma^2$.

6 Generalization Analysis

6.1 Convex Settings

Assumption 4 (β -smooth) $\forall \mathbf{x}, \mathbf{y} \in \Re^d$ and $z \in \mathcal{Z}$, we have $\|\nabla f(\mathbf{x}, z) - \nabla f(\mathbf{y}, z)\| \leq \beta \|\mathbf{x} - \mathbf{y}\|$. It also implies $f(\mathbf{x}, z) - f(\mathbf{y}, z) \leq \langle \nabla f(\mathbf{y}, z), \mathbf{x} - \mathbf{y} \rangle + \frac{\beta}{2} \|\mathbf{x} - \mathbf{y}\|^2$.

Assumption 5 (L -Lipschitz) $\forall \mathbf{x} \in \Re^d$ and $z \in \mathcal{Z}$, we have $\|\nabla f(\mathbf{x}, z)\| \leq L$. It also implies that $\forall \mathbf{x}, \mathbf{y} \in \Re^d$, $|f(\mathbf{x}, z) - f(\mathbf{y}, z)| \leq L \|\mathbf{x} - \mathbf{y}\|$.

Theorem 4 (*Convex generalization error of RSGD-scale*) Assume $f(\cdot, z)$ is convex and Assumptions 4 and 5 exist. If the learning rate $\gamma_t \leq \frac{2}{\beta}$, RSGD-scale has uniform stability with $\epsilon_{RSGD} \leq \frac{2L^2}{N} \sum_{t=0}^{T-1} (1 - (1-\alpha)^{T-t}) \gamma_t$.

Remark 4.1 For SGD in convex settings, the uniform stability satisfies $\epsilon_{SGD} \leq \frac{2L^2}{N} \sum_{t=0}^{T-1} \gamma_t$ (Theorem 3.8 in [8]). The factor $(1 - (1-\alpha)^{T-t})$ in Theorem 4 helps RSGD-scale achieve a better upper bound than SGD.

6.2 Non-Convex Settings

Let S and $S'^{(i)}$ be two sample datasets of size N differing in only one sample. Let \mathbf{x} and \mathbf{x}' be the parameters that we train using a randomized learning algorithm on S and $S'^{(i)}$ respectively.

Theorem 5 (*Non-convex generalization error of RSGD-scale*) Assume $f(\cdot, z)$ is non-convex and Assumption 4 and 5 exist. Then RSGD-scale has uniform stability with $\epsilon_{RSGD} \leq \sum_{t=0}^{T-1} [1 - (1-\alpha)^{T-t-1}] \cdot [\frac{2\gamma_t L^2}{N} + (1 - \frac{1}{N}) \gamma_t \beta L \mathbb{E} \|\mathbf{x}_{t-\frac{1}{2}} - \mathbf{x}'_{t-\frac{1}{2}}\|]$.

Remark 5.1 For SGD in non-convex settings, the uniform stability satisfies $\epsilon_{SGD} \leq \sum_{t=0}^{T-1} \frac{2\gamma_t L^2}{N} + \sum_{t=0}^{T-1} (1 - \frac{1}{N}) \gamma_t \beta L \mathbb{E} \|\mathbf{x}_{t-\frac{1}{2}} - \mathbf{x}'_{t-\frac{1}{2}}\|$ (Proposition 3 in [31]). The factor $[1 - (1-\alpha)^{T-t-1}]$ in Theorem 5 helps RSGD-scale achieve a better upper bound than SGD. We do not make assumption on the learning rate $\gamma_t \leq \frac{c}{t}$ as in the Theorem 3.12 in [8].

Trade-off For the scaling scheme, a proper α slows down the growth rate of the generalization error to improve the generalization with trivial penalties on the convergence performance. It balances the loss surface shift in Figure 2 towards the testing minimum, which has a smaller generalization error than the training minimum. But as $\alpha \rightarrow 0^+$, $c_2 \rightarrow 0^+$ and the error bound in Corollary 3.1 explodes, making it hard to converge. It is due to that the right side of the loss in Figure 2 has low generalization error but poor training and testing performance. In the experiments we choose $\alpha \geq \frac{1}{16}$.

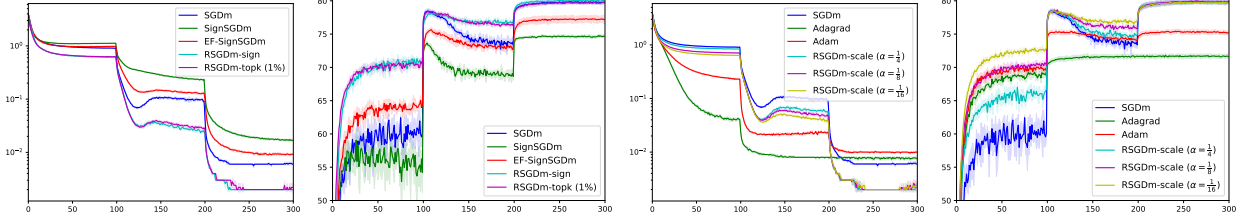


Figure 3: CIFAR-100 training with DenseNet-121. From left to right: training loss, testing accuracy (%), training loss and testing accuracy (%). X-axis denotes the epochs.

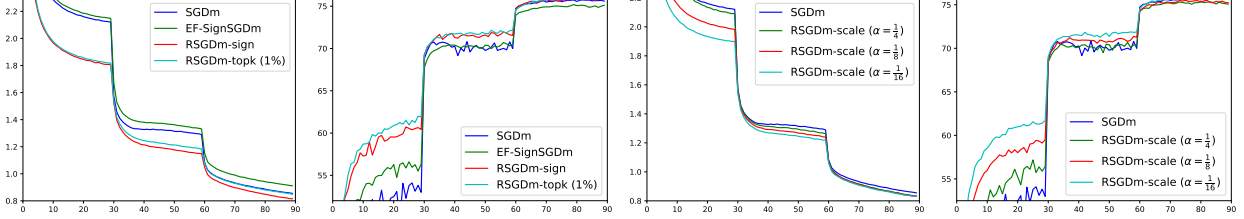


Figure 4: ImageNet training with ResNet-50. From left to right: training loss, validation top-1 accuracy (%), training loss and validation top-1 accuracy (%). X-axis denotes the epochs.

7 Experimental Results

7.1 Experiment Settings

We implement all experiments in PyTorch [22] and run on a cluster with Nvidia Tesla P40 GPUs. We compare the following methods:

- SGD(m), ASGD, Adagrad and Adam.
- SignSGD(m): Gradient compression with scaled sign quantization (Eq. 1).
- EF-SignSGD(m): error feedback for gradient compression with scaled sign quantization.
- RSGD(m)-(sign, top-k, scale): The proposed method with corresponding residual schemes. We also applied our technique to ASGD and Adam.

Image Classification on CIFAR-100 We test DenseNet-121 [11] with growth rate $k = 32$ and GoogLeNet [28] on CIFAR-100 [17] over 5 runs. Data augmentation includes random cropping, random flipping and standardization. We train each model for 300 epochs, with a learning rate decay of 0.1 at epoch 100 and 200. The momentum constant is 0.9 for SGDm-related methods. The base learning rate is 0.1 and the batch size is 128. The weight decay is set to be 0.0005. For Adam/AdaGrad, we select the best base learning rate from $\{1e-2, 5e-3, 1e-3, 5e-4, \dots\}$.

Image Classification on ImageNet We conduct ResNet-18 and ResNet-50 [10] on ImageNet [24]. Data augmentation includes random cropping, random flipping and standardization. We train each model for 90 epochs, with a learning rate decay of 0.1 at epoch 30 and 60. The base learning rate is 0.1. The batch size is 256. The weight decay is 0.0001 and the momentum constant is 0.9.

Word-Level Language Modeling on Penn Treebank We test a 3-layer AWD-LSTM [21] on PTB [20]. The model is trained for 500 epochs with a base learning rate of 30. We follow the public codes¹ for other hyperparameter settings. AWD-LSTM uses the Non-monotonically Triggered ASGD algorithm to automatically switch from SGD optimizer to ASGD [23] optimizer at a certain training step. Correspondingly, we switch from SGD with residuals to ASGD with residuals (RASGD) based on the same criterion. Note that switching will lead to a steep descent of training and validation perplexity (PPL), but different methods may not switch at the same training step.

¹<https://github.com/salesforce/awd-lstm-lm>

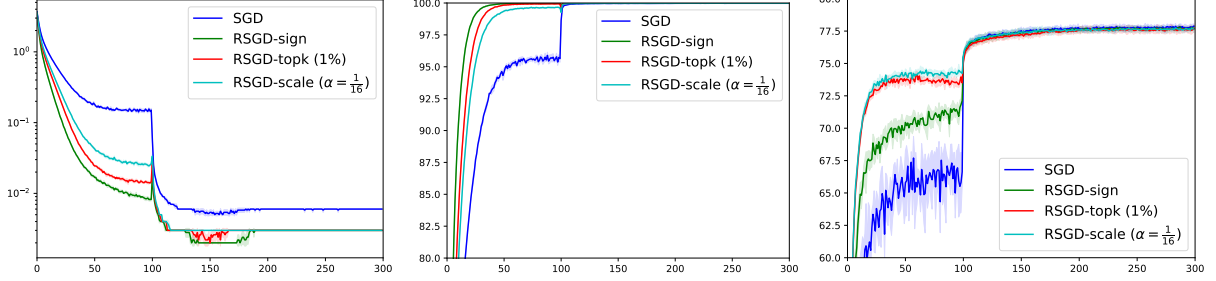


Figure 5: CIFAR-100 training with DenseNet-121 using SGD-related methods. From left to right: training loss, training accuracy (%), testing accuracy (%). X-axis denotes the epochs.

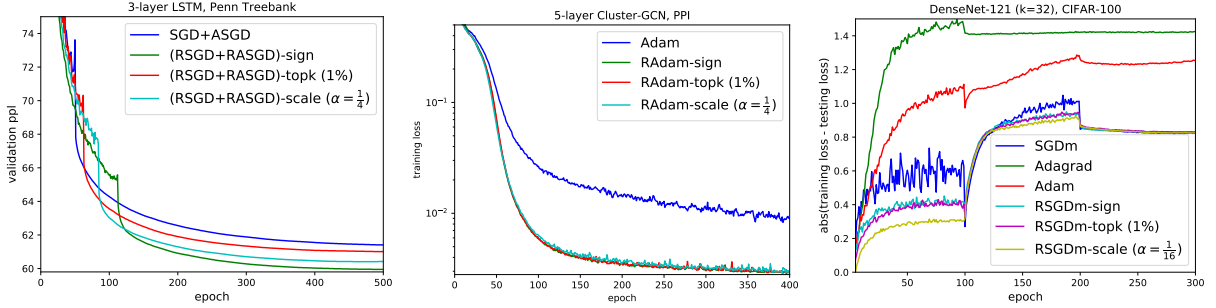


Figure 6: Left: PTB training with AWD-LSTM. Middle: PPI training with Cluster-GCN. Right: generalization error of DenseNet-121 on CIFAR-100.

Graph Convolutional Networks on PPI We apply a 5-layer Cluster-GCN on PPI. The number of hidden units in each layer is 2048. The model is trained for 400 epochs with a learning rate of 0.02. We follow the public codes² for other hyperparameters settings.

7.2 Performance Comparisons

Figure 3 illustrates the training curves of DenseNet-121 on CIFAR-100 with SGDm-related methods, while Figure 5 visualizes the training curves with SGD-related methods. Figure 4 shows the training curves of ResNet-50 on ImageNet. Figure 6 plots the training curves of AWD-LSTM on PTB and Cluster-GCN on PPI. The corresponding metrics are summarized in Tables 1 and 2.

One step to improve the testing accuracy by 16%. As shown in Table 1, the best top-1 testing accuracy of RSGDm outperforms SGDm by 16% at epoch 0-99 for GoogLeNet. In terms of the validation accuracy of the ImageNet experiments, the best top-1 accuracy can be improved by up to 7.9% at epoch 0-29 for ResNet-50. The improvement only requires one simple computation: $\mathbf{x}_{t+1} = \mathbf{x}_t - \mathcal{R}(\mathbf{x}_t - \mathbf{x}_{t+\frac{1}{2}})$ (the re-descent step in Algorithm 1). The residual scheme \mathcal{R} as we explored in this paper is cheap to calculate. Consequently, RSGD(m) can exploit the SGD(m) trajectory for a better performance at no extra cost of gradient evaluation.

Faster and Better than SGD(m)/Adam. As shown in Figure 3, the training loss of RSGDm is smaller than SGDm. Although the training loss is larger than Adam/Adagrad, we witness a better testing performance than Adam/Adagrad/SGDm. The testing curves of RSGD(m) also show a much smaller variance caused by stochastic sampling. As for SignSGDm, there is a large performance loss. EF-SignSGDm compensates for it but without performance gain in the single-worker environment. Similar experimental findings can be drawn from CIFAR-100 experiments without momentum (Figure 3), the large scale ImageNet experiments (Figure 4), the AWD-LSTM and the Cluster-GCN experiments (Figure 6). These experiments validate that RSGD(m) is general to be applied to different deep learning tasks. For the AWD-LSTM experiments, the validation and testing PPL can be improved by 1.20 and 1.04 respectively using RSGD + RASGD. Although the training step of switching optimizer is different, the performance is better both before and after switching.

²https://github.com/google-research/google-research/tree/master/cluster_gcn

Table 1: Top-1 Accuracy (%) on CIFAR-100/ImageNet. Top 1% for topk and $\alpha = \frac{1}{16}$ for scaling.

CIFAR-100		DenseNet-121			GoogLeNet	
Epoch	0-99	100-199	200-299	0-99	100-199	200-299
SGD	67.70±1.65	77.78±0.29	77.88±0.18	66.32±1.14	77.38±0.25	77.39±0.21
RSGD-sign	72.13±0.72	77.70±0.15	77.82±0.18	72.24±0.48	77.18±0.29	77.25±0.34
RSGD-topk	74.15±0.25	77.66±0.21	77.82±0.24	73.73±0.25	77.32±0.19	77.37±0.27
RSGD-scale	74.50±0.14	77.85±0.24	77.89±0.15	74.27±0.27	77.36±0.24	77.35±0.18
SGDm	62.43±0.42	78.49±0.28	79.87±0.26	57.28±3.24	78.88±0.25	80.00±0.24
RSGDm-sign	71.31±0.34	78.11±0.33	80.16±0.22	70.64±0.83	78.28±0.27	80.14±0.28
RSGDm-topk	70.83±0.60	78.40±0.19	79.77±0.14	71.40±0.31	78.93±0.18	79.97±0.22
RSGDm-scale	72.88±0.38	78.49±0.18	79.88±0.13	73.43±0.28	79.00±0.16	79.95±0.14
Adagrad	69.37±0.32	71.72±0.35	71.82±0.33	68.79±0.37	69.67±0.46	69.67±0.46
Adam	70.33±0.39	75.41±0.31	75.45±0.31	67.94±0.51	74.62±0.24	74.79±0.42
ImageNet		ResNet-18			ResNet-50	
Epoch	0-29	30-59	60-89	0-29	30-59	60-89
SGDm	49.33	64.99	70.08	54.10	70.81	75.76
RSGDm-sign	54.80	66.12	70.03	60.72	71.95	76.05
RSGDm-topk	52.89	66.10	69.93	62.00	72.16	76.08
RSGDm-scale	55.82	66.01	69.98	61.72	71.88	75.90

Better Generalization Error. We plot the generalization error of DenseNet-121 on CIFAR-100 in the right of Figure 6. The generalization error of RSGDm grows slower than SGDm/Adam/Adagrad. But as the training steps T grows and the learning rate γ_t decays, the improvement over SGDm becomes less significant, which supports Theorem 5.

Table 2: Validation/Testing PPL of AWD-LSTM.

PTB dataset	PPL
SGD + ASGD	61.41 / 58.89
(RSGD + RASGD)-sign	60.21 / 57.85
(RSGD + RASGD)-topk (1%)	61.01 / 58.64
(RSGD + RASGD)-scale ($\alpha = 1/4$)	60.39 / 58.26

7.3 Proximity

We further look into the size of the proximity that RSGD(m) exploits - that is how far the RSGD(m) trajectory are from the SGD(m) trajectory. Experiments on CIFAR-100 with DenseNet-121 shows that the normalized L_1 distance $\|\mathbf{x}_{t+1} - \mathbf{x}_{t+\frac{1}{2}}\|_1 / \|\mathbf{x}_{t+\frac{1}{2}}\|_1$ between RSGDm-scale ($\alpha = \frac{1}{16}$) and SGDm trajectory is of magnitude 10^{-2} , 10^{-3} and 10^{-4} at learning rate 0.1, 0.01 and 0.001 respectively. As the learning rate decays, the size of the proximity becomes smaller. Changing the parameters by less than 1% can benefit SGDm significantly. It verifies that there is a much better solution very close to the SGDm trajectory. RSGDm provides such a way to find it.

8 Conclusion

We bring up a novel problem of how to exploit the solution trajectory to achieve better generalization and convergence. To address this problem, we propose a novel RSGD(m) algorithm to improve SGD(m) by exploiting the SGD(m) trajectory using residuals. RSGD(m) shows the same (but empirically better) convergence rate and a slower growth rate of generalization error compared with SGD. Experiments on various deep learning tasks show that RSGD(m) significantly improves SGD(m) during training. Other potential residual schemes except scaling, scaled sign and top-k may remain to be further studied.

References

- [1] A. F. Aji and K. Heafield. Sparse communication for distributed gradient descent. *arXiv preprint arXiv:1704.05021*, 2017.
- [2] D. Alistarh, T. Hoefler, M. Johansson, N. Konstantinov, S. Khirirat, and C. Renggli. The convergence of sparsified gradient methods. In *Advances in Neural Information Processing Systems*, pages 5973–5983, 2018.

- [3] J. Bernstein, Y.-X. Wang, K. Azizzadenesheli, and A. Anandkumar. signsgd: Compressed optimisation for non-convex problems. *arXiv preprint arXiv:1802.04434*, 2018.
- [4] J. Bernstein, J. Zhao, K. Azizzadenesheli, and A. Anandkumar. signsgd with majority vote is communication efficient and fault tolerant. *arXiv*, 2018.
- [5] O. Bousquet and A. Elisseeff. Stability and generalization. *Journal of machine learning research*, 2(Mar):499–526, 2002.
- [6] W.-L. Chiang, X. Liu, S. Si, Y. Li, S. Bengio, and C.-J. Hsieh. Cluster-gcn: An efficient algorithm for training deep and large graph convolutional networks. In *Proceedings of the 25th ACM SIGKDD International Conference on Knowledge Discovery & Data Mining*, pages 257–266, 2019.
- [7] J. Duchi, E. Hazan, and Y. Singer. Adaptive subgradient methods for online learning and stochastic optimization. *Journal of Machine Learning Research*, 12(Jul):2121–2159, 2011.
- [8] M. Hardt, B. Recht, and Y. Singer. Train faster, generalize better: Stability of stochastic gradient descent. *arXiv preprint arXiv:1509.01240*, 2015.
- [9] H. He, G. Huang, and Y. Yuan. Asymmetric valleys: Beyond sharp and flat local minima. In *Advances in Neural Information Processing Systems*, pages 2549–2560, 2019.
- [10] K. He, X. Zhang, S. Ren, and J. Sun. Deep residual learning for image recognition. In *Proceedings of the IEEE conference on computer vision and pattern recognition*, pages 770–778, 2016.
- [11] G. Huang, Z. Liu, L. Van Der Maaten, and K. Q. Weinberger. Densely connected convolutional networks. In *Proceedings of the IEEE conference on computer vision and pattern recognition*, pages 4700–4708, 2017.
- [12] P. Izmailov, D. Podoprikhin, T. Garipov, D. Vetrov, and A. G. Wilson. Averaging weights leads to wider optima and better generalization. *arXiv preprint arXiv:1803.05407*, 2018.
- [13] S. P. Karimireddy, Q. Rebjock, S. U. Stich, and M. Jaggi. Error feedback fixes signsgd and other gradient compression schemes. *arXiv preprint arXiv:1901.09847*, 2019.
- [14] N. S. Keskar, D. Mudigere, J. Nocedal, M. Smelyanskiy, and P. T. P. Tang. On large-batch training for deep learning: Generalization gap and sharp minima. *arXiv preprint arXiv:1609.04836*, 2016.
- [15] D. P. Kingma and J. Ba. Adam: A method for stochastic optimization. *arXiv preprint arXiv:1412.6980*, 2014.
- [16] B. Kleinberg, Y. Li, and Y. Yuan. An alternative view: When does SGD escape local minima? In J. Dy and A. Krause, editors, *Proceedings of the 35th International Conference on Machine Learning*, volume 80 of *Proceedings of Machine Learning Research*, pages 2698–2707, Stockholm Sweden, 10–15 Jul 2018. PMLR.
- [17] A. Krizhevsky, G. Hinton, et al. Learning multiple layers of features from tiny images. Technical report, Citeseer, 2009.
- [18] I. Kuzborskij and C. H. Lampert. Data-dependent stability of stochastic gradient descent. *arXiv preprint arXiv:1703.01678*, 2017.
- [19] Y. Lin, S. Han, H. Mao, Y. Wang, and W. J. Dally. Deep gradient compression: Reducing the communication bandwidth for distributed training. *arXiv preprint arXiv:1712.01887*, 2017.
- [20] M. Marcus, B. Santorini, and M. A. Marcinkiewicz. Building a large annotated corpus of english: The penn treebank. 1993.
- [21] S. Merity, N. S. Keskar, and R. Socher. Regularizing and optimizing lstm language models. *arXiv preprint arXiv:1708.02182*, 2017.
- [22] A. Paszke, S. Gross, F. Massa, A. Lerer, J. Bradbury, G. Chanan, T. Killeen, Z. Lin, N. Gimelshein, L. Antiga, et al. Pytorch: An imperative style, high-performance deep learning library. In *Advances in Neural Information Processing Systems*, pages 8024–8035, 2019.
- [23] B. T. Polyak and A. B. Juditsky. Acceleration of stochastic approximation by averaging. *SIAM journal on control and optimization*, 30(4):838–855, 1992.
- [24] O. Russakovsky, J. Deng, H. Su, J. Krause, S. Satheesh, S. Ma, Z. Huang, A. Karpathy, A. Khosla, M. Bernstein, A. C. Berg, and L. Fei-Fei. ImageNet Large Scale Visual Recognition Challenge. *International Journal of Computer Vision (IJCV)*, 115(3):211–252, 2015.
- [25] S. U. Stich. Local SGD converges fast and communicates little. In *International Conference on Learning Representations*, 2019.

- [26] S. U. Stich, J.-B. Cordonnier, and M. Jaggi. Sparsified sgd with memory. In *Advances in Neural Information Processing Systems*, pages 4447–4458, 2018.
- [27] N. Strom. Scalable distributed dnn training using commodity gpu cloud computing. In *Sixteenth Annual Conference of the International Speech Communication Association*, 2015.
- [28] C. Szegedy, W. Liu, Y. Jia, P. Sermanet, S. Reed, D. Anguelov, D. Erhan, V. Vanhoucke, and A. Rabinovich. Going deeper with convolutions. In *Proceedings of the IEEE conference on computer vision and pattern recognition*, pages 1–9, 2015.
- [29] T. Tieleman and G. Hinton. Lecture 6.5-rmsprop: Divide the gradient by a running average of its recent magnitude. *COURSERA: Neural networks for machine learning*, 4(2):26–31, 2012.
- [30] J. Wangni, J. Wang, J. Liu, and T. Zhang. Gradient sparsification for communication-efficient distributed optimization. In *Advances in Neural Information Processing Systems*, pages 1299–1309, 2018.
- [31] Y. Yan, T. Yang, Z. Li, Q. Lin, and Y. Yang. A unified analysis of stochastic momentum methods for deep learning. *arXiv preprint arXiv:1808.10396*, 2018.
- [32] T. Yang, Q. Lin, and Z. Li. Unified convergence analysis of stochastic momentum methods for convex and non-convex optimization. *arXiv preprint arXiv:1604.03257*, 2016.
- [33] S. Zheng, Z. Huang, and J. T. Kwok. Communication-efficient distributed blockwise momentum sgd with error-feedback. *arXiv preprint arXiv:1905.10936*, 2019.